ARTICLE

OBC
www.rsc.org/obc

Electrospray mass spectrometric and DFT study of substituent effects in Ag^+ complexation to polycyclic aromatic hydrocarbons (PAHs)†

Kenneth K. Laali,*[a] Scott Hupertz,‡[a] Alice G. Temu‡[a] and Sergio E. Galembeck*[b]

[a] *Department of Chemistry, Kent State University, Kent, OH, 44242, USA. E-mail: klaali@kent.edu; Fax: 330-6723816; Tel: 330-6722988*

[b] *Departamento de Quimica, Faculdade de Filosofia, Ciencias e Letras de Ribeirao Preto, Universidade de Sao Paulo, Av. Bandeirantes, 3900, Ribeirao Preto, SP, Brazil*

Received 1st March 2005, Accepted 27th April 2005
First published as an Advance Article on the web 16th May 2005

Complexation of Ag(I) cation to a series of substituted anthracenes (AN), phenanthrenes (PH), pyrenes (PY) and cyclopenta[*a*]phenanthrenes (CPaPH) was studied in competitive experiments by allowing PAHs to react in pairs with AgOTf. The resulting complexes were examined by electrospray mass spectrometry (ES-MS) to determine relative abundances of the corresponding monomeric and dimeric complexes. Based on this data a sequence of complexation ability rankings was derived for each group. Among the substituents examined, a -COMe group when placed at the *meso* position in AN and PH, or at the C-1 in PY is most effective in Ag^+ complexation, whereas an $-NO_2$ group is least efficient. Methyl groups at the *meso* positions are better than in the terminal rings. For the CPaPH series, bay region substitution (methyl and alkoxy) have limited effect as does carbonyl substitution in the annelated CP ring. In the PY series, a -COPh or a -CH(Me)OH group at C-1 is as efficient as -COMe. Based on extensive potential energy searches, four types of complexation modes were identified by B3LYP/LANL2DZ calculations involving Ag^+ complexation to $-NO_2$ oxygens, to -COMe or to -OH and a *peri*-carbon, to just one ring carbon, or by bridging two ring carbons. Among these modes, the first two are most favorable. The energetic preferences were rationalized with charge decomposition analysis (CDA). Effect of Ag^+ complexation on relative aromaticity in various rings was examined by NICS (nucleus independent chemical shift) in two representative cases. Structures and energies of the acetyl pyrene–Ag^+–pyrene hetero-dimer and acetyl pyrene–Ag^+–acetyl pyrene homo-dimer complexes were determined with the same model. These complexes have sandwich structures.

Introduction

Structure–activity relationships and substituent effect studies have played an important role in understanding the PAH activation mechanisms,[1] and it has been established for several classes of PAHs that not only structural/conformational effects but also "correct substitution" could strongly impact mutagenic potency and the extent of PAH–DNA adduct formation.[1–8] The importance of cation–π interactions as a noncovalent force in chemistry, biology, and in molecular recognition and host–guest chemistry is well realized.[9–12] Its recognition as a contributing force in biological systems, has prompted extensive model studies, for example, with peptides,[13] cyclophanes,[14] calixarenes,[15] and with lariat ethers,[16] employing alkali metal cations, silver(I) cations, and ammonium salts including acetyl choline. The nature of cation–π interactions has also been examined by theoretical and mass spectrometric studies.[17–22] Given the abundance of metal ions in biological systems, it is conceivable that cation–π complexation could influence the outcome of the oxidative steps leading to metabolic activation of PAHs, or the subsequent events (such as π-stacking and π–π interactions) leading to intercalation into DNA and covalent bonding. However, to our knowledge, allowance has not been made for such interactions and consequences thereof in relation to the accepted mechanistic schemes for PAH activation, *i.e.* diol–epoxide formation leading to the PAH-carbocation and/or electron transfer leading to PAH-radical cation.[2,3,6] Complexation of Li^+ with representative polycyclic arenes has been studied by DFT and FT-ICR.[17] It was found that π-bonds to highly fused inner rings are weaker than the outer π-complexes and that increasing the number of fused cycles reduces the activation barriers which connect various local minima. Although PAH–Ag^+ π-complexes seem less relevant to biology and more related to materials chemistry and crystal engineering, availability of a number of previous investigations on the solid state structures of Ag^+–polyaromatic ligands,[23] solution NMR demonstration of PAH–Ag^+ complexation with large PAHs including the geodesic analogues,[24] and gas phase studies in particular by electrospray-MS showing that these complexes are easily detectable,[25,26] provided confidence and became the impetus for the present model study to examine substituent effects in PAH–Ag^+ complexation in competitive experiments in several classes of PAHs that have been studied extensively in relation to bio-activation and metabolism. The choice of the substituents (alkyl, acetyl, nitro, carbinol *etc.*) and the PAH structures studied were based on a combination of factors including known biological activity in certain cases, presence of various sites for metal ion complexation, steric issues within a class, and the availability of a group of compounds within each class.

Results and discussion

Study domain and procedures

Competitive complexation experiments were carried out with anthracene, phenanthrene, pyrene, and cyclopenta[*c*]phenanthrene derivatives, whereby two differently substituted PAHs,

† Electronic supplementary information (ESI) available: The ES-MS derived data in competitive complexation experiments with anthracene, phenanthrene and pyrene series (where $PAH_1 = M_1$ and $PAH_2 = M_2$). Representative MS-MS spectra for hetero-dimers **1**–Ag^+–**2, 3**–Ag^+–**4, 2**–Ag^+–**5, 4**–Ag^+–**5** and **5**–Ag^+–**3** in the anthracene series, and for **6**–Ag^+–**7, 6**–Ag^+–**8, 7**–Ag^+–**8, 6**–Ag^+–**9** in the phenanthrene series. The ES-mass spectrum of **10**–Ag^+–**15** under low and high skimmer voltage. Xantheas energetic analysis table, table with superposition results and optimized geometries and harmonic vibrational frequencies for all compounds studied computationally. See http://www.rsc.org/suppdata/ob/b5/b503084f/

‡ KSU undergraduate research students.

DOI: 10.1039/b503084f

typically from the same class, were allowed to compete in reaction with AgOTf. The resulting complexes were directly analyzed by ES-MS to determine the relative abundances of PAH_1–Ag^+ and PAH_2–Ag^+ complexes and their ratios. The ES-MS measurements were performed under two sets of conditions: (a) with low skimmer voltage, for which the homo- and hetero-dimer complexes (PAH_1–Ag^+–PAH_1; PAH_2–Ag^+–PAH_2 and PAH_1–Ag^+–PAH_2) are detected along with the monomeric complexes (PAH_1–Ag^+ and PAH_2–Ag^+), and (b) with high skimmer voltage condition, when the hetero-dimers are wiped out and only the monomeric π-complexes are observed (see Experimental section for more details).

Anthracene **1** and substituted anthracenes **2–5**, with acetyl-, nitro- and methyl(s) substituents at the *meso*-position(s) (Fig. 1), and phenanthrene **6** and substituted phenanthrenes **7–9** (Fig. 2) having substituents at the *meso* and in the outer rings were chosen.

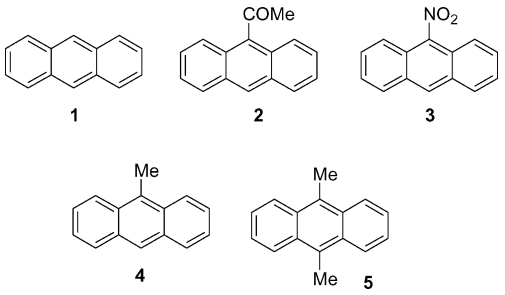

Fig. 1 Anthracene and selected substituted derivatives.

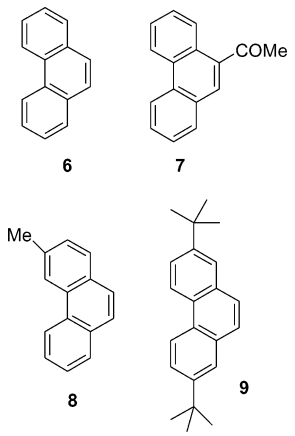

Fig. 2 Phenanthrene and selected substituted derivatives.

In addition, parent pyrene **10**, substituted pyrenes **11–14**, and hexahydropyrene **15** (Fig. 3) were included in the ES-MS study, together with another group of substituted pyrenes **16–20** (Fig. 4) with trifluoromethyl carbinol-, fluoro- and

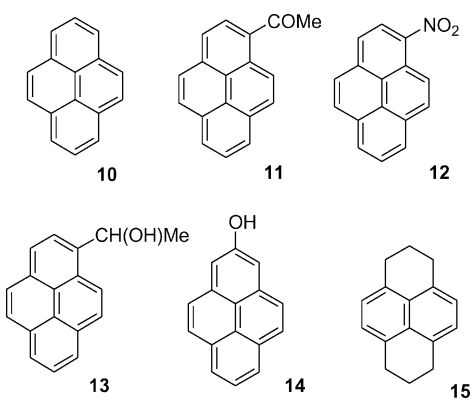

Fig. 3 Pyrene and selected substituted derivatives.

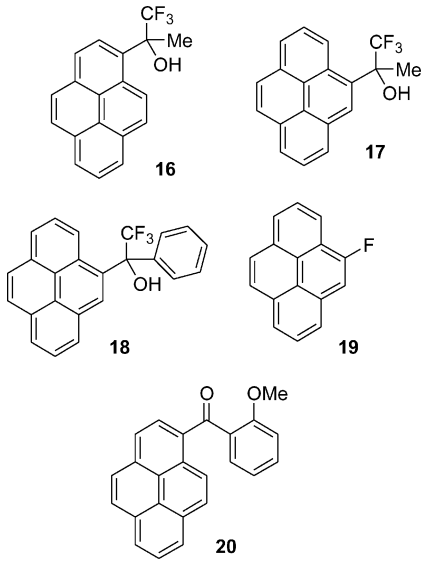

Fig. 4 Additional substituted pyrene derivatives.

benzoyl-substitutents. For the cyclopenta[*a*]phenanthrene series, parent **21** and its derivatives **22–28**, and for comparison 3-acetylphenanthrene **29** (Fig. 5), with substituents at the bay- or non-bay positions and possessing varied degrees of biological activity were included.[27]

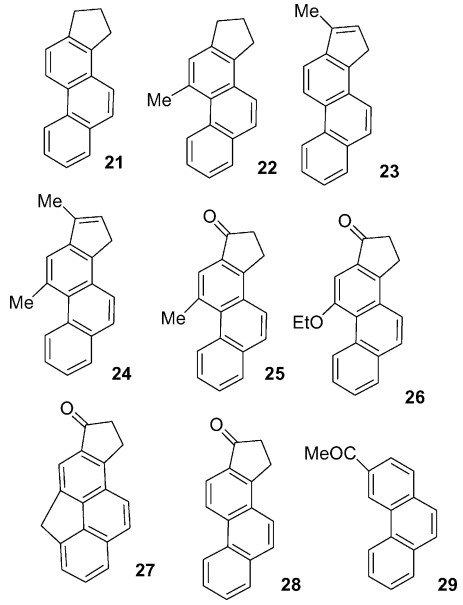

Fig. 5 Cyclopenta[*a*]phenanthrene and selected derivatives.

The relative abundances of these complexes were used to derive relative substituent effects on Ag^+ complexation.

Whenever possible, MS-MS experiments were used to confirm the identity of the Ag^+ adducts. The MS-MS experiments on the hetero-dimers were used as an additional gauge of substituent effect on relative complexation stability [eqn. (1)]:

$$PAH_1\text{–}Ag^+\text{–}PAH_2 \twoheadrightarrow PAH_1\text{–}Ag^+ \textit{ vs } PAH_2\text{–}Ag^+ \qquad (1)$$

Compounds listed in Fig. 6 were selected for DFT study which included an extensive potential energy surface search to identify various complexation modes as a function of the substituent and their relative energies. In selected cases, relative aromaticity in various rings in a given PAH–Ag^+ complex was determined by NICS to gauge the influence of Ag^+ attachment. The DFT work included a study of **10**–Ag^+–**11** and **11**–Ag^+–**11** dimer complexes. In relation to the ES-MS data, an important issue to address by DFT was whether the hetero- and homo-dimer complexes were

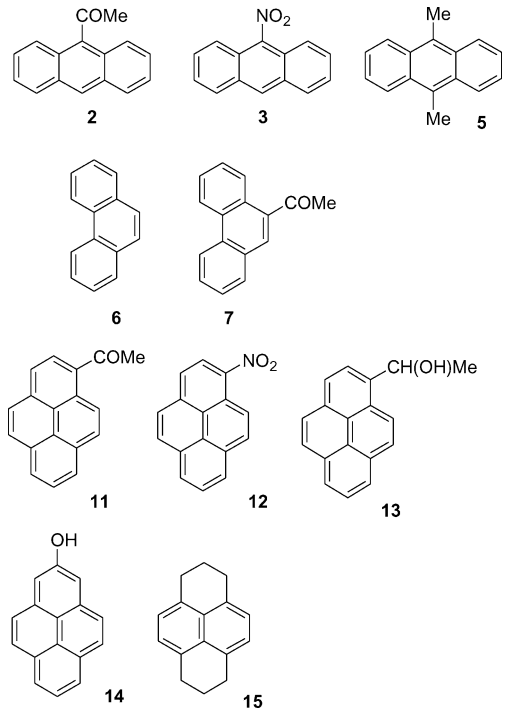

Fig. 6 PAHs selected for DFT study.

sandwich type "PAH_1–Ag^+–PAH_2", or π-stacked "Ag^+–PAH_1–PAH_2".

The ES-MS data and typical spectra

Complexation of Ag^+ to individual PAH substrates was examined first. The spectra consisted of abundant PAH–Ag^+–PAH and PAH–Ag^+ complexes and minor ions due to PAH–Ag^+–H_2O complexes and in some cases minor fragment ions depending on the PAH structure. Increasing the skimmer voltage (20 V → 33 V) led to disappearance of the dimer complexes.

Typically, each spectrum contained the following species: homo- and hetero-dimer complexes (M_1–Ag^+–M_1, M_2–Ag^+–M_2 and M_1–Ag^+–M_2), the monomeric complexes (M_1–Ag^+ and M_2–Ag^+), and the minor $Ag^+ \cdot H_2O$ complexes (M_1–Ag^+–H_2O and M_2–Ag^+–H_2O). Selected ES-MS derived data in competitive complexation experiments for anthracene, phenanthrene and pyrene series (compounds **1–15**) are summarized in the supporting information file (where $PAH_1 = M_1$ and $PAH_2 = M_2$).†

In the anthracene series (Fig. 1), 9-acetylanthracene **2** is most efficient in complex formation, whereas 9-nitroanthracene **3** is least effective relative to other substituents. The following two cases are mentioned as illustrative examples: the MS-MS on 9-acetylanthracene–Ag^+–9-methylanthracene hetero-dimer **2**–Ag^+–**4** at *m/z* 519 (Fig. 7a) produces only the *m/z* 327 ion (**2**–Ag^+) (with **4**–Ag^+ at *m/z* 301 being absent), whereas MS-MS on anthracene–9-nitroanthracene hetero-dimer **1**–Ag^+–**3** (Fig. 7b) produces both the *m/z* 332 ion (**3**–Ag^+) and the *m/z* 287 ion (**1**–Ag^+) with the latter being considerably more abundant.

Representative MS-MS spectra for the hetero-dimers **1**–Ag^+–**2,3**–Ag^+–**4,2**–Ag^+–**5,4**–Ag^+–**5** and **5**–Ag^+–**3** are collected in supporting information (SI) file.† Overall, the following sequence of substituent effect may be derived for the anthracene series:**2** > **4** ~ **5** > **3**.

For the phenanthrene series (Fig. 2), Ag^+ complexation to 9-acetylphenanthrene **7** was strongly preferred relative to **6** and **8, 6** was preferred relative to **9**, and **6** *versus* **8** were about equal. The MS-MS spectra for the corresponding hetero-dimers are collected in the SI file for comparison. It can be seen that MS-MS on *m/z* 479 (**6**–Ag^+–**8**) produced both *m/z* 301 (**8**–Ag^+) and *m/z* 287 (**6**–Ag^+) with the former being more abundant, but the MS/MS on *m/z* 521 (**7**–Ag^+–**8**) gave only **7**–Ag^+. Interestingly, whereas in competitive reactions, **6** complexed more efficiently than **9** (possibly a reflection of steric hindrance by the tBu groups), the MS-MS spectrum of the hetero-dimer complex (*m/z* 577) exhibited a very prominent *m/z* 399 ion due to **9**–Ag^+, with little or no *m/z* 287 ion being detected (**6**–Ag^+). Overall, the following sequence of substituent effect could be derived for the phenanthrene series: **7** > **6** ~ **8** > **9**.

In the pyrene series, compounds **10–15** (in Fig. 3), 1-acetylpyrene **11** complexed most efficiently, whereas 1-nitropyrene **12** was least effective. A β-hydroxy group (as in **13**) was more effective than a conjugated-OH (as in **14**) for Ag^+ complexation. In fact, an OH group at the 2-position had a negative impact, as **10** was more efficient that **14**. A surprising finding was the observation that in hexahydropyrene–pyrene competition the former was better. As illustrative examples, the electrospray mass spectrum of **10**–Ag^+–**15** under low and high skimmer voltage are included in the supporting information file.†

The following sequence of substituent effects on Ag^+ complexation could be derived with this series based on competitive experiments:

11 > **13** > **15** > **10** > **14** > **12**

Turning our attention to the fluorinated (trifluoromethyl carbinols and fluoropyrene) as well as the benzoyl carbinol derivatives**16–20** (see Fig. 4), the most effective substrates for Ag^+ complexation based on ES-MS data *via* competitive experiments were **18** and **20**. Whereas compound **18** was more effective than **16, 18** and **20** had similar complexation tendencies. A competitive experiment between **20** and **11** inferred that the former is at least as reactive.

Finally in the CPaPH series, compounds **21–28** (see Fig. 5), **21** and **22** had rather similar complexation tendencies, **22** was slightly better than **24**, and **26** and **25** were rather similar. A competitive experiment between **21** and **6** established a modest preference for **21**. There was also a modest preference for **29** relative to **25**. But there was a large preference for **7** relative to **25**.

Comparative discussion of the complexation patterns

On the basis of the ES-MS derived data the following points can be made. In the anthracene series, presence of an acetyl group at the *meso*-position has a significant impact on Ag^+ complexation. Replacing the 9-COMe with 9-NO_2 greatly reduces the complexation tendency relative to other anthracenes examined. Complexation tendencies of **4** and **5** are rather similar which implies that introduction of the second methyl group into the *meso* position had little effect, but at the same time, the MS-MS data indicate that the resulting Ag^+–**5** complex is stronger than the Ag^+–**4** complex.

Among the phenanthrenes, the best candidate is **7** with the -COMe group at the *meso* position. A methyl in the 3-position does not have an impact. While presence of two -tBu groups at the 2- and 7-positions diminishes the tendency for complexation; the MS-MS data suggest that once formed, the resulting complex is stronger as compared to phenanthrene itself. Combining the preferences observed for the phenanthrene series with those found for the cyclopenta[*a*]phenanthrenes leads to the assertion that the bay-region may not be involved in Ag^+ complexation. Presence of an acetyl substituent has a major impact only when it is placed on the middle ring. This is clearly manifested in comparing **7** with **25**.

Focusing on the pyrene skeleton, presence of an acetyl group at C-1 is best for Ag^+ complexation, followed by a β-hydroxy group (as in **13**), but a conjugated -OH at C-2 (**14**) is not favorable. A benzoyl substituent at C-1 (as in **20**) is an equally suitable ligand, comparable to 1-acetyl. Additionally, a β-OH ligand with -Ph and CF_3 appends (as in **18**) creates a favorable

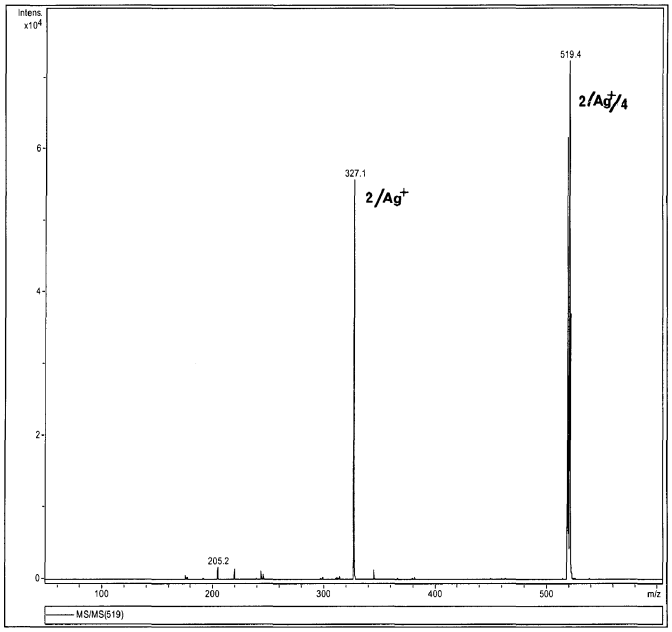

(a)

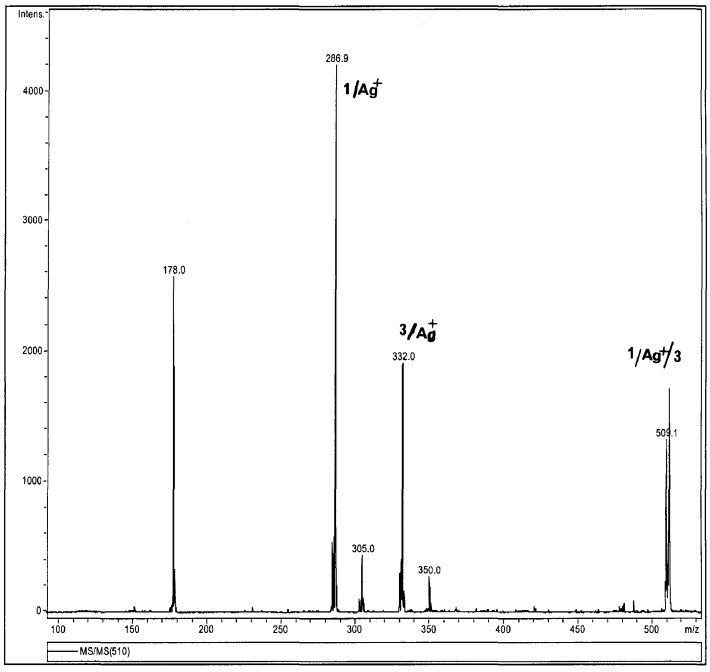

(b)

Fig. 7 a: MS/MS spectrum of **2**–Ag^+–**4** hetero-dimer complex. b: MS-MS spectrum of **1**–Ag^+–**3** hetero-dimer complex.

set up for Ag^+ complexation. Taken together, the α-carbonyl group in the *meso* position of anthracene and phenanthrene, and at the C-1 of pyrene create the most suitable arrangements for Ag^+ complexation.

We then turned our attention to DFT to explore the most favored structures for these complexes.

Computational study

Anthracenes **2, 3**, and **5**, phenanthrenes **6** and **7**, and pyrenes **11–15** were included in the computational study. An extensive potential energy surface search for these substrates indicated that Ag^+ can complex these substrates by four different patterns (Fig. 8). For the nitro derivatives **3** and **12** binding to both nitro oxygens generates a very stable complex (see Table 1) (referred to by designation **3**-OO and **12**-OO). For the acetyl derivatives **2,7** and **11** and for the carbinol **13** stable complexes are formed by Ag^+ complexation to the acetyl oxygen or a carbinol oxygen and a *peri*-carbon (referred to by designations **2**-C_1O, **7**-C_1O, **11**-$C_{10}O$, and **13**-$C_{10}O$ respectively). Other much less stable complexation modes involve one ring carbon (referred to by designations **5**-C_9, **14**-C_6, **14**-C_3, **12**-C_6 and **15**-C_4) or by bridging between two carbons (referred to *via* designations **5**-C_1C_2, **14**-C_4C_5, **12**-C_4C_5, **6**-C_9C_{10}, **6**-C_1C_2, and **6**-C_3C_4).

Tables 1 and S1 present the energy data for the complexes that are within 2 kcal mol^{-1} from the global minimum for each complex, except for 1-nitropyrene (**12**) where energy for all four different patterns of binding are presented. The data illustrate that the **3**-OO and **12**-OO complexes are most stable followed closely by the acetyl complexes in particular **11**-$C_{10}O$, **2**-C_1O, and **7**-C_1O. Complexes where the metal ion is complexed with the π-system are less stable than those that involve oxygen coordination, by more than 10 kcal mol^{-1}. Finally, there seems to be no clear preference for complexation modes involving one

Table 1 Relative binding energy, ΔE_B, (kcal mol^{-1}), for Ag^+–PAH complexes

	$\Delta(\Delta E_B)$
(**12**-OO)	0.00
(**3**-OO)	1.23
(**11**-C_{10}O)	2.95
(**7**-C_1O)	3.21
(**2**-C_1O)	3.31
(**13**-C_{10}O)	10.57
(**5**-C_1C_2)	12.53
(**15**-C_4)	12.73
(**12**-C_{10}O)	13.33
(**14**-C_6)	14.45
(**5**-C_9)	14.57
(**14**-C_3)	15.54
(**14**-C_4C_5)	15.64
(**6**-C_9C_{10})	16.37
(**6**-C_3C_4)	17.18
(**6**-C_1C_2)	17.34
(**12**-C_6)	24.37
(**12**-C_4C_5)	26.29

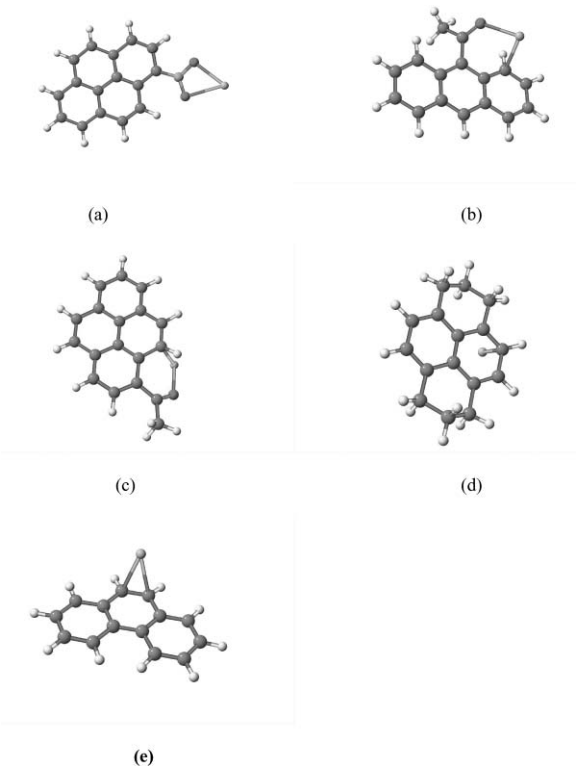

Fig. 8 Four patterns of the interaction between Ag^+ and studied PAHs: (a) (12-OO), (b) (2-C_1O) (c) (11-C_{10}O), (d) (15-C_4), (e) (6-C_9C_{10}).

ring carbon or bridging between two ring carbons. However, there are some discrepancies in these patterns. The relative stability of **13**-C_{10}O and **12**-C_{10}O are much lower than **11**-C_{10}O, whereas those of **2**-C_1O, and **7**-C_1O are similar, as are π-complexes such as **5**-C_1C_2 and **15**-C_4. For **13**-C_{10}O, this can be ascribed to the smaller negative charge of carbinol oxygen as compared to carbonyl oxygen. But, **12**-C_{10}O seems to present an anomalous behavior. All attempts to find an electronic or structural cause were unsuccessful, indicating the need for further studies.

The most stable complexes involve the interaction of Ag^+ with the most electronegative atoms, as in nitro-PAH complexes that involve complexation with two oxygens, and the least stable forms was produced by complexation with π-system of aromatic carbons. The relative stability is independent of the model, as indicated in Table 2 for various complexes of Ag^+ with **12**. Results for SDD PP (pseudo potential) are very similar to

Table 2 Relative binding energy, ΔE_B, (kcal mol^{-1}), for complexation of Ag^+ with **12**

	LANL2DZ	SDD	MIXB[a]
(**12**-OO)	0.00	0.00	0.00
(**12**-C_{10}O)	13.33	13.33	9.57
(**12**-C_6)	24.37	24.31	18.12
(**12**-C_4C_5)	26.29	26.01	19.86

[a] MIXB: LANL2DZ for Ag and 6-31+G(d,p) for main group atoms.

LANL2DZ PP. The use of this PP for Ag and 6-31+G(d,p) basis set for the main group elements only reduces the relative stability as compared with LANL2DZ or SDD. The geometries of the complexes optimized by these three models are very similar, as indicated by the superposition of structures (the root mean square of the differences in the position of all atoms is in the order of 10^{-2} Å) (Table S2).

The observed stability appears to be contrary to expectation based on the HSAB (hard and soft acids and bases) principle. As Ag^+ is a soft ion, the most favored site should be an aromatic carbon that presents the highest HOMO electronic density. In order to understand the reason(s) for this behavior, charge decomposition analysis (CDA), originally proposed by Dapprich and Frenking was used.[28] This method is a quantitative implementation of Dewar–Chatt–Duncanson (DCD) model to interpret chemical bonding in transition metal complexes[29] and has been used by several authors in recent years.[30] Table 3 presents the data from CDA analysis for complexes of **12**, assuming that the PAH is the donor. As can be seen from the first entry of this table, a correlation between donation and stability is observed only for the three least stable complexes, **12**-C_{10}O, **12**-C_4C_5 and **12**-C_6. All these complexes have at least one π bond with the metal. In contrast, **12**-OO, is a σ-complex. From the paper of Bruce and Rocha it is possible to observe a correlation between donation and stability of mixed Fe(II) phosphametallocenes, that are π complexes.[30a] The lack of correlation between donation and stability can be explained by the observation of Hernandez *et al.* that CDA does not present the proper balance between σ-donation and π-back-donation for CO chemisorbed in transition metals.[30b] The back-donation decreases and the relative donation/back-donation increases with the stability of the complexes, indicating that back-donation destabilizes the complexes and the stability of the complexes are given by the balance between donation and back-donation. The energetic decomposition analysis indicates that this interaction cannot be explained by the hardness (χ). The quality of CDA approach can be verified by the small residual term and by the agreement between relative energy of binding (ΔE[B]) calculated by CDA and Xantheas method.

Table 4 presents NICS for **11**-C_{10}O and **12**-OO for comparison (see also Fig. 10). Several authors in recent years used NICS in PP calculated wavefunctions to study the aromaticity of ligands in transition metal complexes, with very consistent results.[31] Comparing NICS(1) for both systems, the aromaticity in the

Table 3 Summary of the charge decomposition analysis for all complexes between Ag^+ and **12**. Charge terms in electrons and energetic ones in kcal mol^{-1}

	(**12**-OO)	(**12**-C_{10}O)	(**12**-C_6)	(**12**-C_4C_5)
Σ donation	0.432	0.481	0.377	0.340
Σ back donation	−0.001	0.030	0.045	0.050
Σ repulsion	−0.095	−0.117	−0.079	−0.079
Σ residual	−0.013	−0.022	−0.007	−0.030
$\Sigma d/\Sigma b$	−432.00	16.03	8.38	6.80
μ	−250.65	−166.83	−158.97	−158.44
χ	476.51	265.56	316.85	337.75
E[B]	65.92	52.40	39.88	37.16
ΔE[B]	0.00	13.52	26.04	28.76

Table 4 NICS (ppm) calculated by B3LYP/LANL2DZ

	(**11**-C_{10}O)		(**12**-OO)	
Ring[a]	NICS(0)	NICS(1)	NICS(0)	NICS(1)
A	−7.89	−2.57	−3.27	−5.77
B	−9.78	−6.20	−3.08	−6.21
C	−11.47	−1.65	−3.40	−6.68
D	−6.04	−11.78	−6.00	−9.17

[a] See Fig. 10. [b] For benzene, NICS(0) = −6.75 and NICS(1) = −9.85

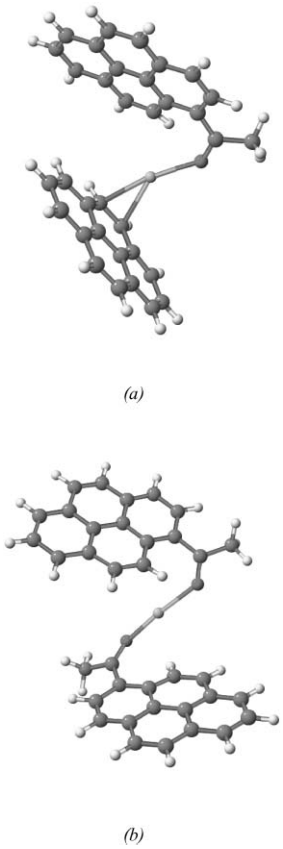

Fig. 9 Structure of the sandwich complexes: (a) 1-acetylpyrene-Ag^+-pyrene. (b) 1-acetylpyrene-Ag^+–1-acetylpyrene.

B-ring does not change as a result of Ag^+ complexation. The C-ring in **11**-C_{10}O is most affected by complexation and is not aromatic any more. This is not the case for **12**-OO. Aromaticity in the substituent-bearing A-ring is greatly reduced in **11**-C_{10}O but only to some extent in **12**-OO. Therefore, based on NICS the A/C rings in 1-acetylpyrene–Ag^+ complex are no longer aromatic.

Fig. 9 represents the geometry of the 1-acetylpyrene–Ag^+–pyrene hetero-dimer complex (**11**–Ag^+–**10**) and the homo-dimer **11**–Ag^+–**11**. Only the sandwich complexes are minima and all

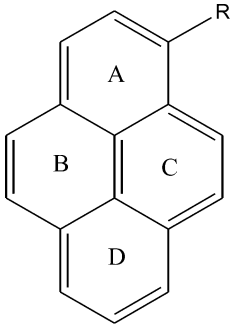

Fig. 10

Table 5 Electronic energy (E), zero-point correction and their sum (Hartree), two-body, BE_2, total, E_B, and relative binding energy, ΔE_B, and basis set superposition error (kcal mol^{-1}) for **11**–Ag^+–**10** **11**–Ag^+–**11** dimer complexes

	(**11**–Ag^+–**10**)	(**11**–Ag^+–**11**)
E	−1529.580506	−1682.215510
ZPE	0.458078	0.494529
E + ZPE	−1529.122428	−1681.720981
$BE_2(a–Ag^+)$[a]	−54.45	−53.26
$BE_2(b–Ag^+)$[a]	−43.38	−54.04
$BE_2(a–b)$[a]	3.13	5.33
E_B	−79.70	−87.99
ΔE_B	8.29	0.00
BSSE	3.94	4.33

[a] *a*: 1-Acetylpyrene, *b*: pyrene for (**11**–Ag^+–**10**) and 1-acetylpyrene for (**11**–Ag^+–**11**).

attempts to obtain a complex in which the metal ion is not sandwiched between the two PAHs were unsuccessful. This can be attributed to unfavorable stacking and by stabilization when both O–Ag^+–π and Ag^+–π interactions can operate in sandwich complex mode (see Fig. 9). From this figure it is possible to observe that both complexes adopt very similar stacked-displaced conformations. It can be seen that in **11**–Ag^+–**10** hetero-dimer, the acetyl pyrene unit is stacked to maximize the interaction between the metal ion and the C_4/C_5 of the pyrene unit. In contrast, in the **11**–Ag^+–**11** homo-dimer, the acetyl pyrene units are displaced and interact mainly *via* the acetyl oxygens and to a lesser extent *via* the C_{10}. The O–Ag^+–O for **11**–Ag^+–**11** is nearly linear, which is one of the most common geometries for Ag^+ complexes.

Table 5 presents the total energies, zero point corrections, BSSE, two body interaction energies BE_2, and total binding energy E_B which is corrected by BSSE. In both dimers there is a small drop in energy for the interaction **11**–Ag^+ compared with (**11**-C_{10}O). The homo-dimer is 8.29 kcal mol^{-1} more stable than the hetero-dimer because the interaction **11**–Ag^+ is stronger than **10**–Ag^+. It is interesting to note that the interaction between both PAHs are repulsive. This helps to understand the preferred conformation, where both rings present a very small overlap. Similarly, for the benzene dimer, a parallel displaced conformation is one of the minima on the potential energy surface.

Comparing the MS data with DFT

Regarding the nitro-PAHs, the complexation mode involving only the nitro oxygens, predicted by DFT to be a very stable mode, is not inferred from competitive solution complexation experiments, which show them to be much less favorable relative to other substituents examined. This implies that alternative mode(s) involving the π-system must be more abundant in solution. The next best complexation mode is for the acetyl derivatives and here the MS-based data and DFT are in agreement. The geometry of this type of complex as determined by DFT involves the acetyl oxygen and a *peri*-carbon. Complexation modes involving the π-system are the next best possibilities and generally this concurs with the outcome of competitive experiments. The structure of these complexes, as computed by DFT, involve Ag^+ complexation to one ring carbon or bridging between two ring carbons, and these modes are almost equally preferred.

NICS for **11**–Ag^+ and **12**–Ag^+ complexes infers that whereas nitro oxygens complexation in **12**–Ag^+ has little impact on the aromaticity of individual rings, the aromaticty of the A/C rings are greatly diminished in **11**–Ag^+ where Ag^+ complexes the acetyl oxygen and the *peri*-carbon.

Finally, concerning the commonly observed dimer complexes and the earlier discussed MS-MS experiments on the hetero-dimers, the remarkable structures of hetero-dimer **11**–Ag^+–**10**

and the homo-dimer complex **11**–Ag^+–**11** have been calculated by DFT. Interestingly, only sandwich complexes are formed and no stable structures in which silver ion is not sandwiched between the two PAH units could be found.

As a next step, we have embarked on model computational studies focusing on complexation of alkali metal ions with the oxidized metabolites (epoxides, dihydrodiols and diol–epoxides) in biologically relevant classes of PAHs, to explore how this might affect subsequent ring opening and carbocation formation.

Experimental

The PAH substrates used in this study were available from previous studies in our laboratory. They were either commercially available or had been synthesized in our lab *via* previously reported procedures.[27,32]

Electrospray-MS measurements were performed on a Bruker Esquire ESI ion-trap mass spectrometer system in the positive ion mode. The following instrument settings were utilized: capillary −4000 V; end plate offset −500 V; nebulizer (N_2) 5.0 psi; dry gas (N_2) 5.00 L min^{-1}; dry temp 250 °C; primary skimmer 20 V/33 V; secondary skimmer 6.0 V; scan range 50–1000 m/z; scan rate 1650 m/z s^{-1}; number of scans 20; syringe pump (Cole/Palmer 74900 series); sample influx rate 2.0 mL min^{-1}.

Complexation studies

a) Single PAH–Ag^+ complexes. Each PAH was allowed to react with AgOTf in MeOH solvent in 1 : 3 equimolar ratio (10 μM PAH: 30 μM AgOTf). After magnetic stirring or sonication, the resulting clear homogeneous solutions were injected into the electrospray instrument *via* an automated syringe pump (2.0 μL min^{-1}). The trap drive and octapoles were optimized towards an m/z range that was an average of all possible complex species (monomeric and dimeric complexes). The potential across the primary skimmer was lowered to 20 eV to allow weakly bound dimer complexes to be observed along with the more stable monomeric complexes. The identity of the PAH–Ag^+ adducts was confirmed by MS-MS.

b) Competitive complexation. A 1 : 1 mixture of two different PAHs from the same class was allowed to react with 3 equivalents of AgOTf in MeOH solvent. Sample introduction method was the same as the single experiments. Spectra were first recorded with the skimmer potential set to 20 V "low voltage method". Subsequently the skimmer potential was raised to 33 V "high voltage method".

Computational methods

Geometry optimization and vibrational frequency calculations were performed with the B3LYP hybrid functional[33] and LANL2DZ PP.[34] This PP uses D95V basis set[35] for the first row and Los Alamos electron core potential (ECP) and double-zeta basis for Na–Bi. Some tests were made with SDD PP, which uses D95V basis up to Ar and Stuttgart/Dresden ECPs on the remainder of the periodic table.[36] Tests were also made for LANL2DZ for Ag and 6-31+G(d,p) for main group atoms. The sites of complexation were determined, for **14**, by starting with Ag^+ perpendicular to every heavy atom at a distance of 2.5 Å (the MP2/Hay-Wadt/6-31G(d) Ag–C bond length for $[Ag(CO)]^{2+}$]).[28] A comparison with HOMO coefficients, NPA (natural population analysis),[37] Mulliken and MK (Merz–Kollmann)[38] charges indicates that only negative MK charges were able to indicate Ag^+ complexation sites. For all other compounds the sites for complexation to Ag^+ were determined *via* electrostatic potential charges (ESP), using the MK distribution of points.[38] The binding energies (ΔE_B) were calculated by Xantheas method.[39] The basis set superposition error (BSSE) was corrected by counterpoise method.[40] For two-body complexes ΔE_B calculated by Xantheas method is equal to the difference of dimer energy with sum of the energies of monomers. NICS was calculated by GIAO (gauge independent atomic orbitals) method.[41] All calculations were performed with Gaussian 03 W software,[42] except CDA analysis that was made with CDA 2.1.2 software.[43] The superposition was made with superpose module of Tinker 4.2 suite of programs.[44] The molecular graphics were created by Jmol v 9 software.[45]

Acknowledgements

The authors acknowledge helpful suggestions from the referees. We thank the Ohio Board of Regents for MS instrumentation grant *via* the Ohio MS consortium for the purchase of the Esquire LC-MS system at KSU. This work was supported in part by the NCI of NIH (# 2 R15 CA078235-02A1). Computational work was supported by Brazilian foundations FAPESP, CAPES and CNPq.

References

1 *Polycyclic Aromatic Hydrocarbon Carcinogenesis: Structure-Activity Relationships*, vol 1–2, S. K. Yang and B. D. Silverman, Ed., CRS Press, Boca Raton, Florida, 1988.
2 *Polycyclic Aromatic Hydrocarbons Chemistry and Carcinogenicity*, R. G. Harvey, Ed., Cambridge University Press, Cambridge, UK, 1991.
3 *Polycyclic Hydrocarbons and Carcinogenesis*, R. G. Harvery, Ed, ACS symposium series 283, ACS, Washington DC, 1985.
4 M. M. Coombs and T. S. Bhatt, *Cyclopenta[a]phenanthrenes*, Cambridge University Press, Cambridge, UK, 1987.
5 W. M. Baird, *Polycyclic Aromat. Compd.*, 2004, **24**, 237.
6 R. G. Harvey and N. E. Geacintov, *Acc. Chem. Res.*, 1988, **21**, 66.
7 N. T. Nashed, S. K. Balani, R. J. Loncharich, J. M. Sayer, D. Y. Shipley, R. S. Mohan, D. L. Whalen and D. M. Jerina, *J. Am. Chem. Soc.*, 1991, **113**, 3910.
8 V. J. Melendez-Colon, A. Luch, A. Seidel and W. M. Baird, *Chem. Res. Toxicol.*, 2000, **13**, 10.
9 J. C. Ma and D. A. Dougherty, *Chem. Rev.*, 1997, **97**, 1303.
10 S. D. Zaric, *Eur. J. Inorg. Chem.*, 2003, 2197.
11 P. Lhotak and S. Shinkai, *J. Phys. Org. Chem.*, 1997, **10**, 273.
12 W. Abraham, *J. Inclusion Phenom. Macrocyclic Chem.*, 2002, **43**, 159.
13 Z. Shi, C. A. Olsen and R. N. Kallenbach, *J. Am. Chem. Soc.*, 2002, **124**, 3284.
14 (*a*) S. Bartoli and S. Roelens, *J. Am. Chem. Soc.*, 2002, **124**, 8307; (*b*) C. A. Hunter, C. M. R. Low, C. Rotger, J. G. Vinter and C. Zonta, *Proc. Nat. Acad. Sci. U. S. A.*, 2002, **99**, 4873.
15 (*a*) K. Araki, H. Hiroyasu and S. Shinkai, *Chem. Lett.*, 1993, 205; (*b*) I. Fumiaki, Y. Miyahara, T. Inazu and S. Shinkai, *Angew. Chem., Int. Ed. Engl.*, 1995, **34**, 1364; (*c*) L. Frish, M. O. Vysotsky, V. Boehmer and Y. Cohen, *Org. Biomol. Chem.*, 2003, **1**, 2011; (*d*) R. Arnecke, V. Boehmer, R. Cacciapaglia, A. Dalla Cort and L. Mandolini, *Tetrahedron*, 1997, **53**, 4901.
16 G. W. Gokel, L. J. Barbour, R. Ferdani and J. Hu, *Acc. Chem. Res.*, 2002, **35**, 878.
17 J.-F. Gal, P.-C. Maria, M. Decouzon, O. Mo, M. Yanez and J. L. M. Abboud, *J. Am. Chem. Soc.*, 2003, **125**, 10394.
18 M. Ashi, F. Mazza and A. Di Nola, *THEOCHEM*, 2002, **587**, 177.
19 F. M. Siu, N. L. Ma and C. W. Tsang, *Chem. Eur. J.*, 2004, **10**, 1966.
20 M. V. Frash, A. C. Hopkinson and D. K. Bohme, *J. Am. Chem. Soc.*, 2001, **123**, 6687.
21 D. Kim, S. Hu, P. Tarakeshwar, K. S. Kim and J. M. Lisy, *J. Phys. Chem. A*, 2003, **107**, 1228.
22 (*a*) S. Tsuzuki, T. Uchimaru and M. Mikami, *J. Phys. Chem. A*, 2003, **107**, 10414; (*b*) M. Yoshida, S. Tsuzuki and N. Tamaoka, *J. Chem. Soc., Perkin. Trans. 2*, 2001, 1021.
23 S. V. Linderman, R. Rathore and J. K. Kochi, *Inorg. Chem.*, 2000, **39**, 5707.
24 R. B. M. Ansems and L. T. Scott, *J. Phys. Org. Chem.*, 2004, **17**, 819.
25 T. Shoeib, A. Cunje, A. C. Hopkinson and K. W. M. Su, *Am. Soc. Mass. Spectrom.*, 2002, **13**, 408.
26 K. M. Ng, N. L. Ma and C. W. Tsang, *Rapid. Commun. Mass. Spectrom.*, 1998, **12**, 1679.
27 K. K. Laali, T. Okazaki and M. M. Coombs, *J. Org. Chem.*, 2000, **65**, 7399; K. K. Laali, S. Hollenstein, S. E. Galembeck and M. M. Coombs, *J. Chem. Soc., Perkin Trans. 2*, 2000, 211.
28 S. Dapprich and G. Frenking, *J. Phys. Chem.*, 1995, **99**, 9352.

29 J. S. Dewar, *Bull. Soc. Chim. Fr.*, 1951, **18**, c79; J. Chatt and L. A. Duncanson, *J. Chem. Soc.*, 1953, 2939.
30 (*a*) E. D. V. Bruce and W. R. Rocha, *Organometallics*, 2004, **23**, 5308; (*b*) G. Frison and H. Grützmacher, *J. Organomet. Chem.*, 2002, **643–644**, 285; (*c*) M. G. Hernández, A. Beste, G. Frenking and F. Illas, *Chem. Phys. Lett.*, 2000, **320**, 222.
31 Q. S. Li and Q. Jin, *J. Phys. Chem. A*, 2004, **108**, 855; Q. S. Li and Q. Jin, *J. Phys. Chem. A*, 2003, **107**, 7869; B. Kiran and M. T. Nguyen, *J. Organomet. Chem.*, 2002, **643–644**, 265; D. J. Tantillo and R. Hoffmann, *Helv. Chim. Acta*, 2001, **84**, 1396; B. Goldfuss and P. v. R. Schleyer, *Organometallics*, 1997, **16**, 1543.
32 K. K. Laali and P. E. Hansen, *J. Org. Chem.*, 1997, **62**, 5804; K. K. Laali, M. Tanaka, S. Hollenstein and M. Chang, *J. Org. Chem.*, 1997, **62**, 7752; K. K. Laali, T. Okazaki and P. E. Hansen, *J. Org. Chem.*, 2000, **65**, 3816.
33 A. D. Becke, *J. Chem. Phys.*, 1993, **98**, 5648.
34 T. H. Dunning, Jr. and P. J. Hay, in *Modern Theoretical Chemistry*, ed. H. F. Schaefer, III, Plenum, Press, New York, 1976, vol. 3, p. 1; P. J. Hay and W. R. Wadt, *J. Chem. Phys.*, 1985, **82**, 270; W. R. Wadt and P. J. Hay, *J. Chem. Phys.*, 1985, **82**, 284; P. J. Hay and W. R. Wadt, *J. Chem. Phys.*, 1985, **82**, 299.
35 T. H. Dunning, Jr. and P. J. Hay, in *Modern Theoretical Chemistry*, Ed. H. F. Schaefer III, Vol. 3, Plenum, New York, 1976, pp. 1–28.
36 X. Y. Cao and M. Dolg, *J. Mol. Struct. (Theochem)*, 2002, **581**, 139 and references cited therein.
37 A. E. Reed, R. B. Weinstock and F. Weinhold, *J. Chem. Phys.*, 1985, **83**, 735.
38 B. H. Besler, K. M. Merz, Jr. and P. A. Kollman, *J. Comput. Chem.*, 1990, **11**, 431; U. C. Singh and P. A. Kollman, *J. Comput. Chem.*, 1984, **5**, 129.
39 S. S. Xantheas, *J. Chem. Phys.*, 1994, **100**, 7523; S. S. Xantheas, *J. Chem. Phys.*, 1996, **104**, 8821; R. L. T. Parreira and S. E. Galembeck, *J. Am. Chem. Soc.*, 2003, **125**, 15615.
40 S. Simon, M. Duran and J. J. Dannenberg, *J. Chem. Phys.*, 1996, **105**, 11024; S. F. Boys and F. Bernardi, *Mol. Phys.*, 1970, **19**, 553.
41 P. v. R. Schleyer, C. Maerker, A. Dransfeld, H. Jiao and N. J. R. Hommes, *J. Am. Chem. Soc.*, 1996, **118**, 6317.
42 M. J. Frisch, G. W. Trucks, H. B. Schlegel, G. E. Scuseria, M. A. Robb, J. R. Cheeseman, J. A. Montgomery, Jr., T. Vreven, K. N. Kudin, J. C. Burant, J. M. Millam, S. S. Iyengar, J. Tomasi, V. Barone, B. Mennucci, M. Cossi, G. Scalmani, N. Rega, G. A. Petersson, H. Nakatsuji, M. Hada, M. Ehara, K. Toyota, R. Fukuda, J. Hasegawa, M. Ishida, T. Nakajima, Y. Honda, O. Kitao, H. Nakai, M. Klene, X. Li, J. E. Knox, H. P. Hratchian, J. B. Cross, C. Adamo, J. Jaramillo, R. Gomperts, R. E. Stratmann, O. Yazyev, A. J. Austin, R. Cammi, C. Pomelli, J. W. Ochterski, P. Y. Ayala, K. Morokuma, G. A. Voth, P. Salvador, J. J. Dannenberg, V. G. Zakrzewski, S. Dapprich, A. D. Daniels, M. C. Strain, O. Farkas, D. K. Malick, A. D. Rabuck, K. Raghavachari, J. B. Foresman, J. V. Ortiz, Q. Cui, A. G. Baboul, S. Clifford, J. Cioslowski, B. B. Stefanov, G. Liu, A. Liashenko, P. Piskorz, I. Komaromi, R. L. Martin, D. J. Fox, T. Keith, M. A. Al-Laham, C. Y. Peng, A. Nanayakkara, M. Challacombe, P. M. W. Gill, B. Johnson, W. Chen, M. W. Wong, C. Gonzalez, and J. A. Pople, *Gaussian 03, Revision A.1*, Gaussian, Inc., Pittsburgh PA, 2003.
43 S. Dapprich, G. Frenking, *CDA 2.1, version 2.1.1*, Marburg, 1995.
44 J. W. Ponder, *Tinker: Software Tools for Molecular Design, version 4.2*, 2004.
45 Jmol-An OpenScience Project © 2004 by Jmol eam.http://jmol.sourceforge.net/.